Visual
Abstract

Estimating degradation of strength of neat PEEK and PEEK-CF laminates under cyclic loading by mechanical hysteresis loops

Alexey Bogdanov

Laboratory of Mechanics of Polymer Composite Materials, Institute of Strength Physics and Materials Science of Siberian Branch of Russian Academy of Sciences, Tomsk, Russia

Department of Materials Science, Engineering School of Advanced Manufacturing Technologies, National Research Tomsk Polytechnic University, Tomsk, Russia

ispmsbogdanov@gmail.com, http://orcid.org/0000-0001-8858-5768

Alexander Eremin, Mikhail Burkov

Laboratory of Mechanics of Polymer Composite Materials, Institute of Strength Physics and Materials Science

ave@ispms.ru, http://orcid.org/0000-0002-1800-9818

burkovispms@mail.ru, http://orcid.org/0000-0002-3337-6579

Sergey Panin

Laboratory of Mechanics of Polymer Composite Materials, Institute of Strength Physics and Materials Science of Siberian Branch of Russian Academy of Sciences, Tomsk, Russia

Department of Materials Science, Engineering School of Advanced Manufacturing Technologies, National Research Tomsk Polytechnic University, Tomsk, Russia

svp@ispms.ru, http://orcid.org/0000-0001-7623-7360

Pavel Lyubutin

Laboratory of Mechanics of Polymer Composite Materials, Institute of Strength Physics and Materials Science of Siberian Branch of Russian Academy of Sciences, Tomsk, Russia

p.lyubutin@gmail.com, http://orcid.org/0000-0003-1732-0791

OPEN ACCESS

ABSTRACT. A DIC-based method was employed for assessing the fatigue induced degradation of mechanical properties of neat polyetheretherketone (PEEK) and its laminated composite reinforced with unidirectional carbon fibers. Its operation principle is based on the remote measurement and calculation of the maximum and minimum strains in a cycle, as well as both dynamic and secant moduli estimated from mechanical hysteresis loops. It is shown that these parameters reflect the degree of material damaging, enabling to predict its current mechanical state.

KEYWORDS. Polyetheretherketone (PEEK), Polymer composite, Fatigue, Elastic modulus, Mechanical hysteresis loop, Digital image correlation.

INTRODUCTION

Polymer composite materials (PCMs) are increasingly used in the aircraft industry due to their both specific strength and corrosion resistance. Recently, interest in the design and application of PCMs based on high strength thermoplastic binders (High Performance Polymers/HPP) has grown significantly [1–3]. On this way, in addition to solving the key technological problems of their fabrication, the task of estimating current strength properties is topical, primarily under cyclic loading.

Since it is extremely important to reveal the development of localized inelastic strains, caused by scattered damage accumulation and microcracking in PCMs during fatigue tests, the issue of implementing such research methods is relevant. Typically, contact crack opening gauges are used for this purpose, but they cannot be implemented or does not provide the required accuracy in some cases (for a number of reasons). As a worthy alternative, non-contact (remote) techniques are well suited, including the digital image correlation (DIC) method, which was deployed for studying laminated fiber (fabric)-reinforced PCMs [4–7].

It is known that laminated reinforced PCMs are designed for operation under severe loads, determined by high strength of reinforcing fibers. Their failure is associated with the gradual damage accumulation at the interfacial/interlayer boundaries due to a significant difference in strength properties of the components. At the same time, laminated high strength fiber-reinforced PCMs (laminates) possess extremely low ductility, greatly limiting the applicability of the DIC method for their examination. Most investigations in this area were devoted to the classification of damage, as well as the analysis of strain fields at the stages preceding their failure [8–10].

Mechanical hysteresis loops, which are one of the key characteristics of fatigue failure, can change their both shape and parameters (depending on the material microstructure) that enables their use for analyzing the behavior of structural materials, including PCM during fatigue testing. The hysteresis loop areas [11], the secant and the dynamic moduli [12] were analyzed by many authors for achieving this goal. For assessing the damage development a reduction in loss tangent (viscoelastic damping factor), width of hysteresis loop, and displacement amplitude, measured in load-controlled fatigue tests may be also applied [13].

For composite materials the dynamic modulus (also called the apparent or tangent modulus) and the secant modulus (also known as fatigue modulus [14,15]) and their degradation rate is often associated with the development of cyclic damage in the specimen and used for predicting fatigue life [16–18]. Although the decrease in both moduli can be induced by damage accumulation, the decrease in the secant modulus is also caused by the development of inelastic deformations (cyclic creep). In doing so, the direct link between damage and secant modulus drop is not straight forward in our case. In turn, the dynamic modulus reflects the stiffness of the specimen, and therefore dynamic modulus characterizes the accumulation of damage that reduced the stiffness.

Most models, describing the hysteresis behavior under cyclic loading, are based on phenomenological approaches and were developed for laminated PCMs [19]. In these methods, the damage accumulation mechanisms were not taken into account, although the corresponding indicators (fatigue stiffness, fatigue strength, residual strength, etc.) were applied to assess their levels. These parameters depend on many factors, including applied loads, fatigue modes, operating durations, cycling load frequencies, environmental conditions, etc. [20].

In this study, a DIC-based method for evaluating strength degradation was utilized and tested for both neat PEEK and its laminated composite reinforced with unidirectional carbon fibers. The investigated parameters were the maximum and minimum strains, their range in a cycle, as well as both dynamic and secant moduli estimated from mechanical hysteresis loops. It was expected that these characteristics should reflect the damage degree, enabling to predict the current mechanical state of the materials. Thus, two opposite cases were considered; near creep behavior being characteristic for low-cyclic fatigue of neat PEEK, while PEEK-CF laminates experienced fatigue behavior close to high-cyclic fatigue mode.

MATERIALS AND METHODS

Two kinds of materials were investigated:
1.   Neat PEEK samples were fabricated from the "PEEK Victrex 450G" powder (Victrex plc) with an average particle size of 16 μm. The hot-pressing temperature was 380 °C, the exposure time under compression molding working pressure of 10 MPa was equal to 30 minutes.

A laminated composite with the "Cetex TC1200" prepreg (Toray), based on a unidirectional tape of the "HexTow AS4D" carbon fibers with a linear density of 12K, as well as 34 wt.% PEEK as a binder. A thickness of the prepreg monolayers was ~0.14 mm. Their laying with a total thickness of 2.2 mm was quasi-isotropic and

symmetrical: [45/0/–45/90]2s. The stack of tapes was laid out in a mold, which was then placed in a thermal press preheated to T=300 °C with a pressure of 1 MPa. After that, it was heated up to T=385 °C with a heating rate of 1.5°C/min, being then held for 10 min at a temperature of 385 °C. Then the mold was cooled down to T=300 °C with a cooling rate of 1.5 °C/min. After that, the pressure was released, while the workpiece was pressed out and then cooled in air down to room temperature.

Structural examinations of neat PEEK were performed using notched samples mechanically fractured after cooling in liquid nitrogen at a temperature of –197 °C for one hour. The cleaved surfaces were utilized for visualization of the bulk structure. A copper film ~10 nm thick was deposited onto the fracture surfaces using a "JEOL JEE-420" vacuum evaporator (JEOL USA, Inc., Peabody, Massachusetts, USA). Their micrographs (Fig. 1) were acquainted with a "LEO EVO 50" scanning electron microscope (SEM; Carl Zeiss, Oberkochen, Germany) at an accelerating voltage of 20 kV.
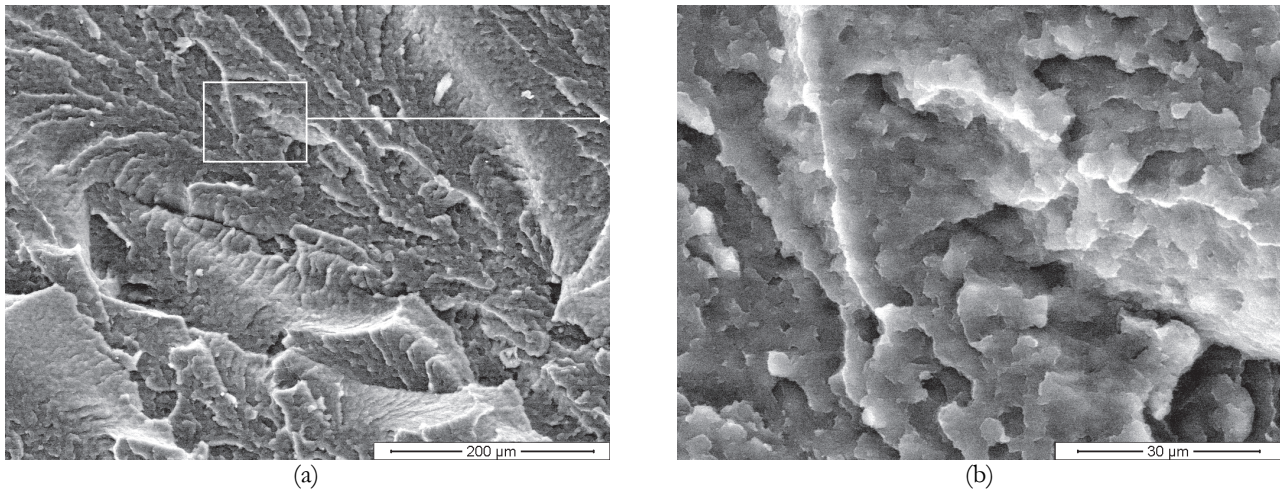

| (a) | (b) |

Figure 1: The SEM micrographs of the cleaved neat PEEK surfaces taken at low (a) and high (b) magnifications.

The structure of the composite was investigated with a "Quanta 200 3D" SEM. Samples were cut from a fabricated workpiece using a polycrystalline diamond end mill. Then, their surfaces were polished with a P2000 grit sandpaper according to ISO 6344. The micrographs are shown in Fig. 2.
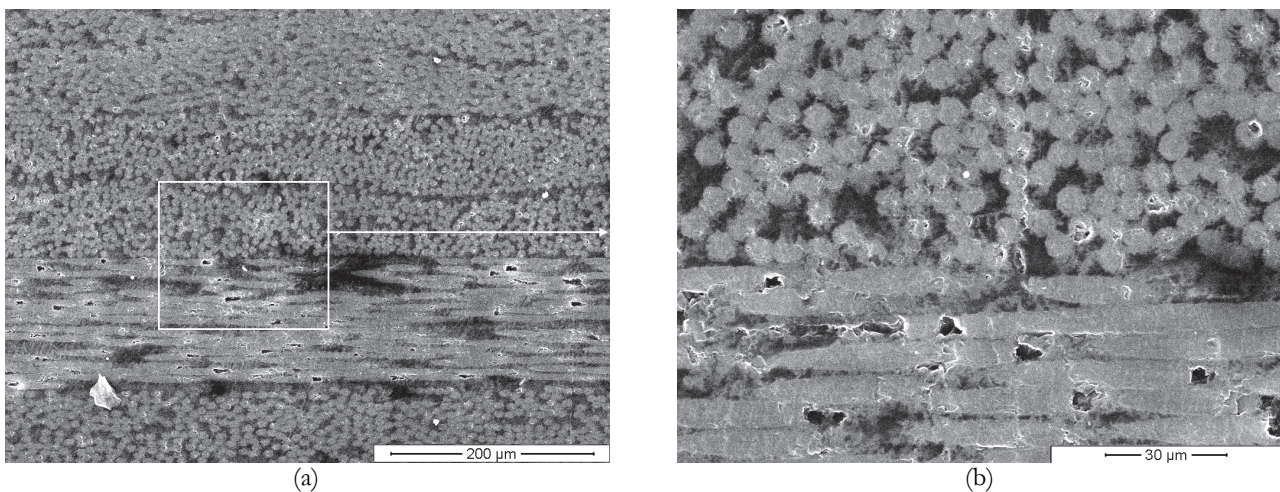

| (a) | (b) |

Figure 2: The SEM micrographs of the laminate composite surfaces at low (a) and high (b) magnifications.

Mechanical tests were carried out with a computer-controlled setup, which included a "BiSS UTM 150 kN" servo-hydraulic machine (Bangalore, India). Strains were assessed by the DIC method. For this purpose, a speckle pattern was deposited on the specimen surfaces using water-based acrylic paint. A solid white color background was sprayed, while randomly located black dots were applied over it with grey color paint [21].

During the tests, the surfaces with speckle patterns were captured using a "PointGrey Grasshopper 50S5M" digital video camera with a matrix size of 2448×2048 pixels at regular time intervals. The surfaces were illuminated with a "Jinbei EF-100 LED Sun Light" diode lamp. A controller connected to a computer via a serial port was used to control the testing machine and a chamber. Both hardware trigger and software developed by the authors were implemented to synchronize the image capturing process with the joint automated operation of the camera and the testing machine. Then, the recorded images were processed using the "VIC-2D" software (Correlated Solutions, USA).

Since the fabrication parameters for neat PEEK and the laminates differed, their structure was examined with the help of the SEMs. Note, that particular defects for neat PEEK might be: porosity, heterogeneity, presence of nonmelted powder particles, while lack of interlayer and interphase adhesion, pores, fiber deviations and heterogeneity of layer stacking might be characteristic flaws for the PEEK-CF laminates. The structure of neat PEEK (fig. 1) was characterized as homogeneous one; no signs of inclusions and porosity were evident. The fracture surface possessed ductile pattern, while neither heterogeneity nor presence of nonmelted powder particles were found.

The SEM micrographs of the PEEK-CF laminate structure are shown in fig. 2. One can see that the fibers were evenly distributed in the polymer; there were neither inclusions nor pores in the matrix. There were no gaps between the prepreg layers as well, which indicates a sufficient level of pressure during samples' manufacturing as well as uniform stacking of the plies.

Static tensile tests of "dog-bone" specimens from neat PEEK (Fig. 3) were performed according to ASTM D638 at a cross-head speed of 1 mm/min and a load sampling frequency of 100 Hz. The number of tested samples was equal to 3.
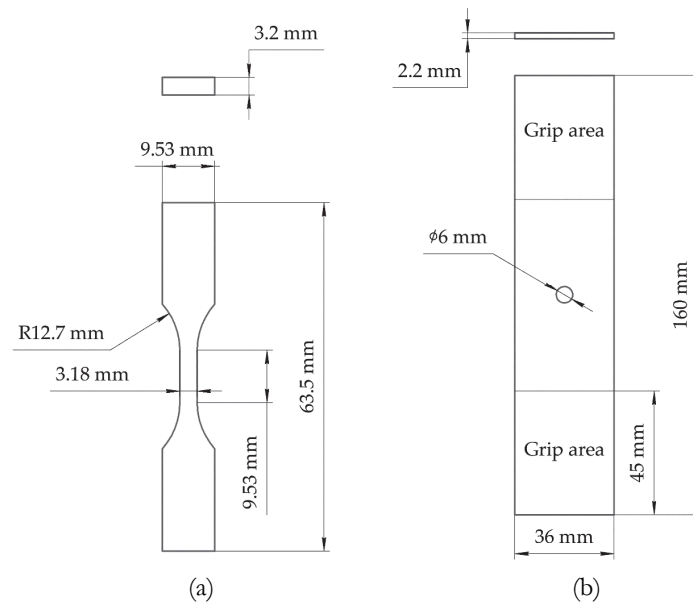

Figure 3: A scheme of the specimens for the static tensile test: "dog-bone" shape specimen for the neat PEEK (a) and open-hole specimen of the PEEK-CF laminate (b).

Static tension tests of the composite were preformed according to ASTM D5766-11 with the "BiSS UTM 150 kN" servo-hydraulic testing machine at a cross-head speed of 1.2 mm/min; the corresponding strain rate was 0.00015 s^{-1}. At least 3 samples were tested. The image capturing was carried out at an image acquisition rate of 1 frame/s. Preliminary static tensile tests of open–hole specimens (with a central hole) made it possible to preset the correct load level in cyclic testing. The shape and dimension of the open–hole samples for both static and fatigue tests were similar.

Fatigue tests of neat PEEK were carried out according to ASTM E606 under the tension and load-control mode at an R ($\sigma_{min}/\sigma_{max}$) stress factor of 0.1 and a sinusoidal load frequency of 1 Hz. The loading data were recorded in real time at a measurement (sampling) frequency of 100 Hz. For assessing strains by the DIC method, the sample surfaces were captured continuously for the first 100 loading cycles and at every 50 cycles after that. So, the image capturing frequency was 0.05 Hz initially, but it increased up to 1 Hz at the final stage. The image capturing process was carried out at a sampling rate of 5 frames/s, recording about 100 images per loop.

Fatigue tests of the composite were carried out according to ASTM D7615 under the tension and load-control mode at the R stress factor of 0.1 and at a load frequency of 5 Hz. For all specimens, the maximum stresses in a cycle were taken equal to 80% of the average value of the ultimate tensile strength of the samples with a central hole. The testing was stopped at 1, 2, 5, 10, 20, 50, 100, 200, 500, 1000, 2000, and 5000 cycles, as well as at 5000 cycles after that until failure (according to

the applied standard). At these points, quasi-static loading and unloading were carried out, capturing the specimen surfaces. In these cases, complete cycle diagrams were recorded. The number of tested samples was equal to 3. All the static and fatigue tests carried out at room temperature.

The recorded load-unload diagrams were the basis for drawing mechanical hysteresis loops for both neat PEEK and its laminated composite, allowing to evaluate their mechanical properties [22]. An analysis of the parameters of each loop make it possible to assess their degradation upon testing. In the current research, both secant and dynamic moduli, the minimum and maximum strains in a cycle, as well as its range were determined. The E_{dyn} dynamic modulus was defined as a slope from the $(\sigma_{max}, \varepsilon_{max})$ maximum point of a hysteresis loop to its $(\sigma_{min}, \varepsilon_{min})$ minimum. The E_{sec} secant modulus was plotted as a slope from zero to the $(\sigma_{max}, \varepsilon_{max})$ maximum point of the hysteresis loop, Fig. 4.

Using the above-described technique and equipment, it was possible to obtain the information on variation in the moduli and residual strains under cyclic loading.
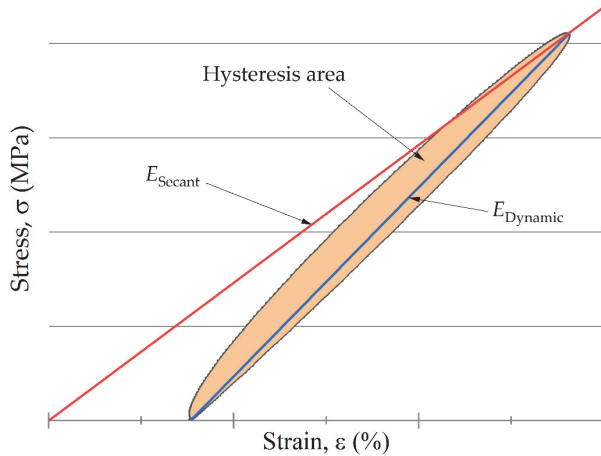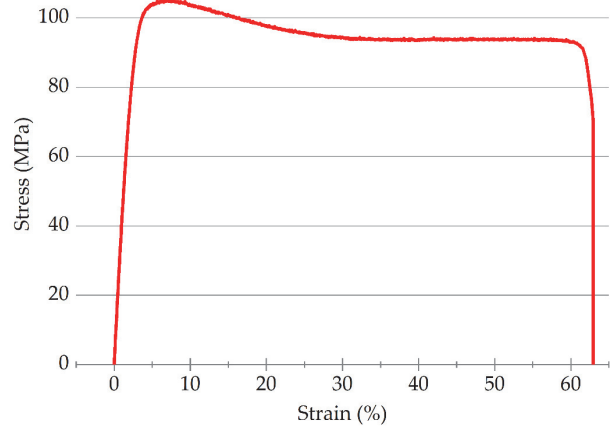

Figure 4: Hysteresis loop parameters.

Figure 5: A typical stress–strain diagram for neat PEEK under the quasi-static tension.

TEST RESULTS FOR NEAT PEEK

Static tension

A stress–strain diagram registered under the static test of neat PEEK is shown in Fig. 5, while its mechanical characteristics are presented in Tab. 1. At the onset of the test, the diagram was almost linear, but it changed into an inelastic (or forced high-elastic type) then. Near the maximum stress (yield strength or forced elasticity), the tangent slope decreased sharply, which was typical of semicrystalline polymers. The maximum stress characterized the formation of a neck. Further rising of strains was associated with the polymer plasticity, i.e., with the conformation of macromolecules. Thus, inelastic strains were predominant (up to 92% of the total level) during the test.

Ultimate tensile strength (MPa)	Elastic modulus (GPa)	Elongation at break (%)	Yield strength 0.2%(MPa)
σ_{UTS}	E	ε_f	$\sigma_{0.2}$
105±1	4.50±0.20	63±5	59.9±0.3

Table 1: The mechanical properties of neat PEEK.

Note that the obtained mechanical properties of neat PEEK agree well with data from the manufacture's datasheet [23].

Cyclic tests

Testing neat PEEK under the cyclic loads enabled to evaluate the development of residual strains (cyclic creep). The tests were carried out at different levels of the maximum load in a cycle: at 0.93 of the ultimate tensile strength ($0.93 \cdot \sigma_{UTS} = 98$ MPa), when the N durability was 400 cycles, and at $0.90 \cdot \sigma_{UTS} = 95$ MPa, when it was 2974 (significantly higher). During the tests, strain ranges almost did not change (they were equal to 3.9% and 3.3%, respectively). Typical load versus strain responses for neat PEEK under fatigue for both load levels are shown in Fig. 6.
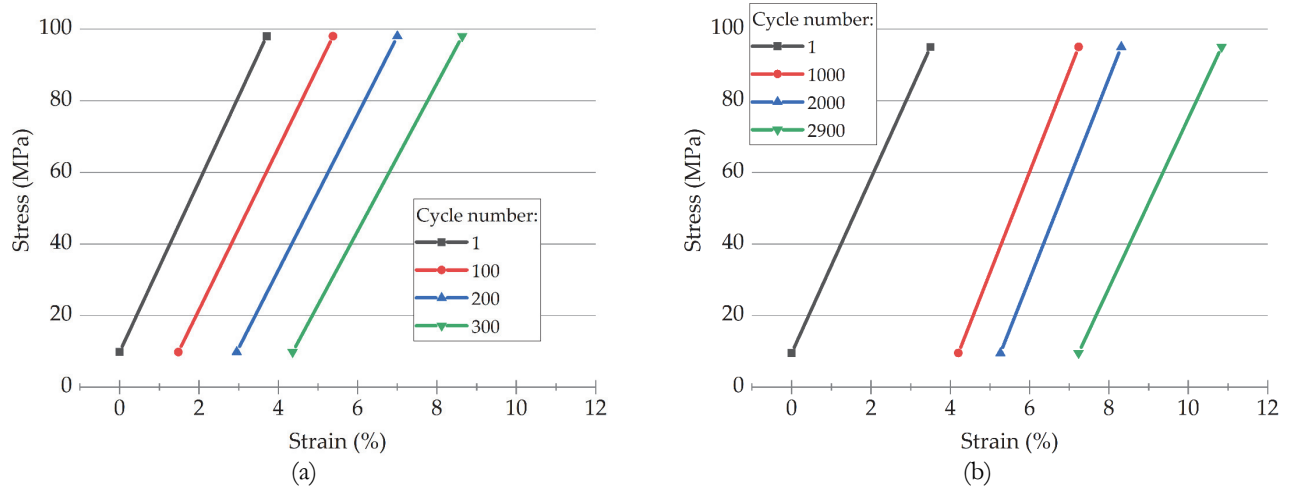
Figure 6: Typical load versus strain responses under fatigue $0.93 \cdot \sigma_{UTS} = 98$ MPa (a), $0.90 \cdot \sigma_{UTS} = 95$ MPa (b) under cyclic loading.
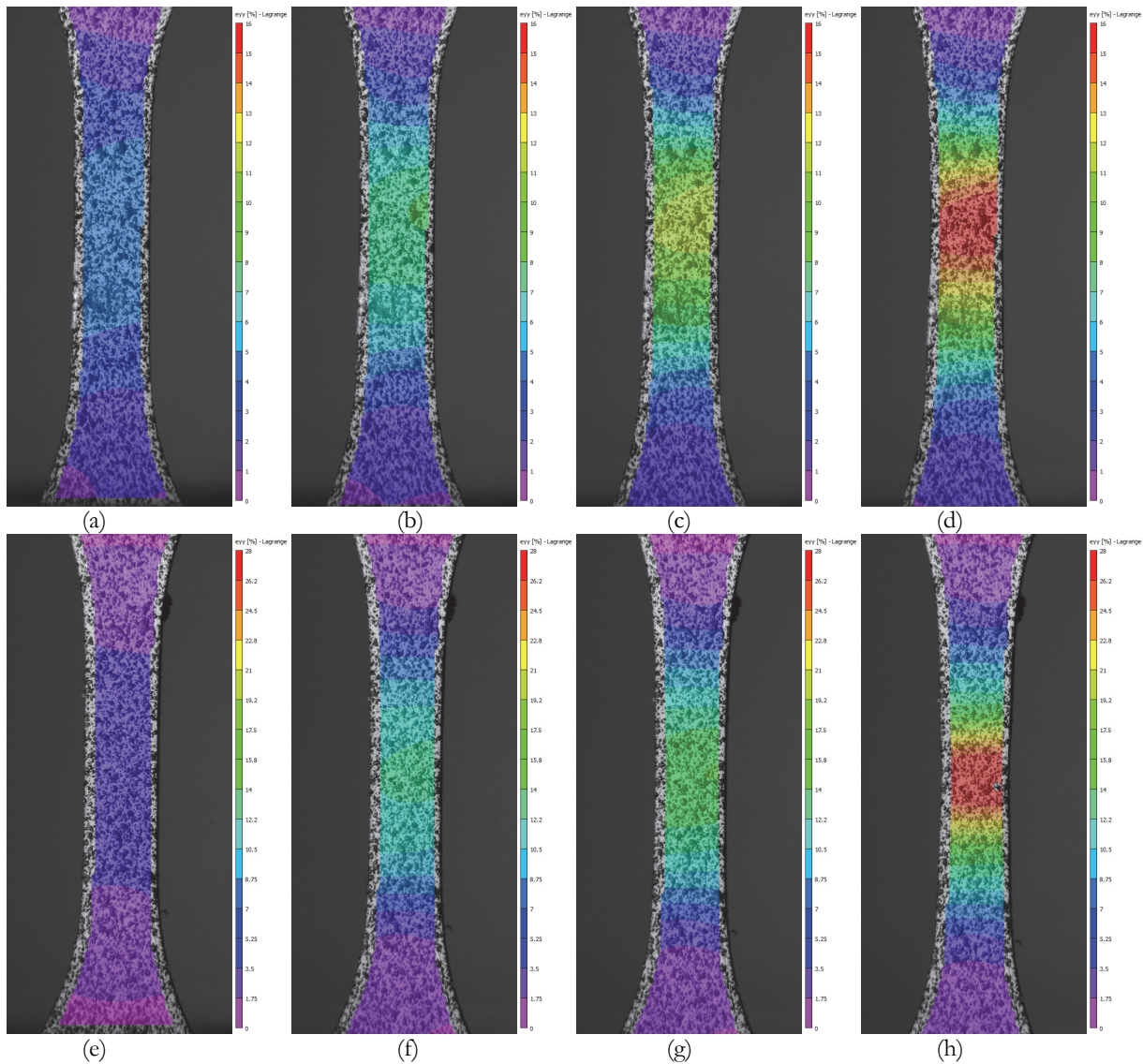

Figure 7: Characteristic patterns of ε_{yy} strain component distribution taken at various number of cycles; neat PEEK at the maximum stress in a cycle of $0.93 \sigma_{UTS}$ (a-d) and $0.90 \sigma_{UTS}$ (e-h); $N = 1$ cycle (a); 100 cycles (b); 200 cycles (c); 300 cycles (d); 1 cycle (e); 1000 cycles (f); 2000 cycles (g); 2900 cycles (h).

The characteristic patterns of εyy strain component distribution taken at maximum cycle stress for various number of cycles are given in Fig. 7.

The comparison of strain distribution patterns shown in Fig. 7 made it possible to conclude the following. In contrast to the mode of 0.90 σ_{UTS} , when failure took place at $N = 2900$ cycles, the strain values were twice as high in the regime of 0.93 σ_{UTS}, when fracture occurred at $N = 400$ cycles.

Creep was assessed by changes in the minimum strains in a cycle. In the first case ($N = 400$ cycles), the minimum strain was 0.2% at the onset of the test. At $N = 300$ cycles (Fig. 8a, curve 1), it was 4.4%, so the residual strain was 4.2%. The creep rate was estimated as $14 \cdot 10^{-3}$ %/cycle. The presented graphs (Fig. 8,a) illustrate typical dependences taken from the results of testing of all samples of each type.

At $N = 2974$ cycles, the minimum strain increased from 0.2% at the onset of the test up to 7.2% by the failure stage. In this case, the creep rate was $2.4 \cdot 10^{-3}$ %/cycle, which was greatly less than the reported above, despite the fact that the stress range changed insignificantly. Curves 1 and 2 in Fig. 8b characterized the typical creep behavior (under low cycle fatigue/LCF conditions).
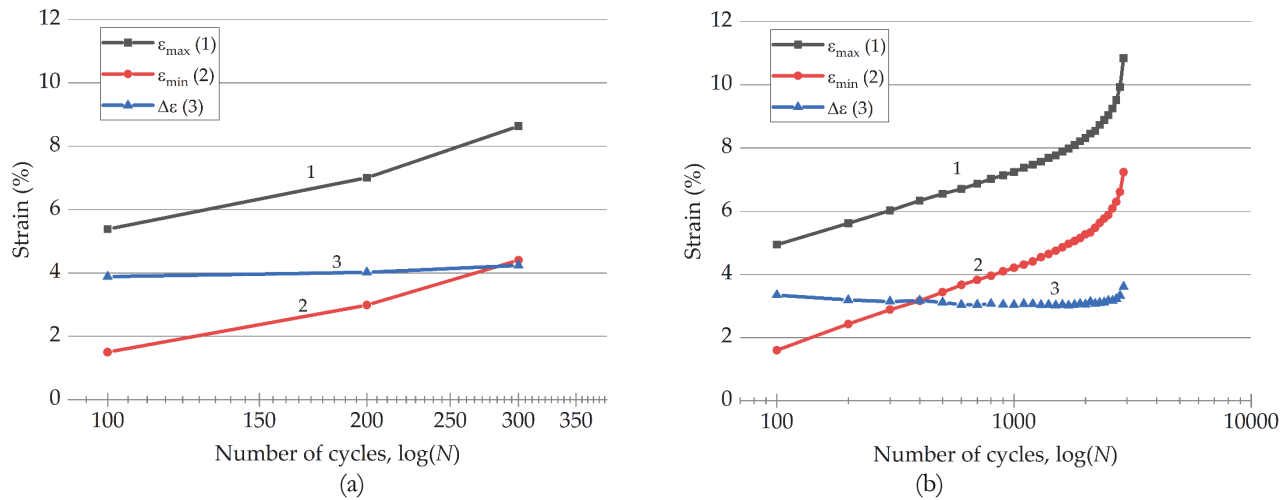

Figure 8: Typical dependences of the maximum (1) and minimum (2) strains, as well as its range (3) versus the number of cycles for neat PEEK at the maximum stains in a cycle of 0.93 σ_{UTS} (a) and 0.90 σ_{UTS} (b).

At the cyclic load mode of $0.90 \cdot \sigma_{UTS} = 95$ MPa, more pronounced creep was evidenced. However, since the strain developed less intensively, the internal structure was able to conform, enhancing the durability. For both cyclic loads, changes in the dynamic and secant moduli are shown in Fig. 9.
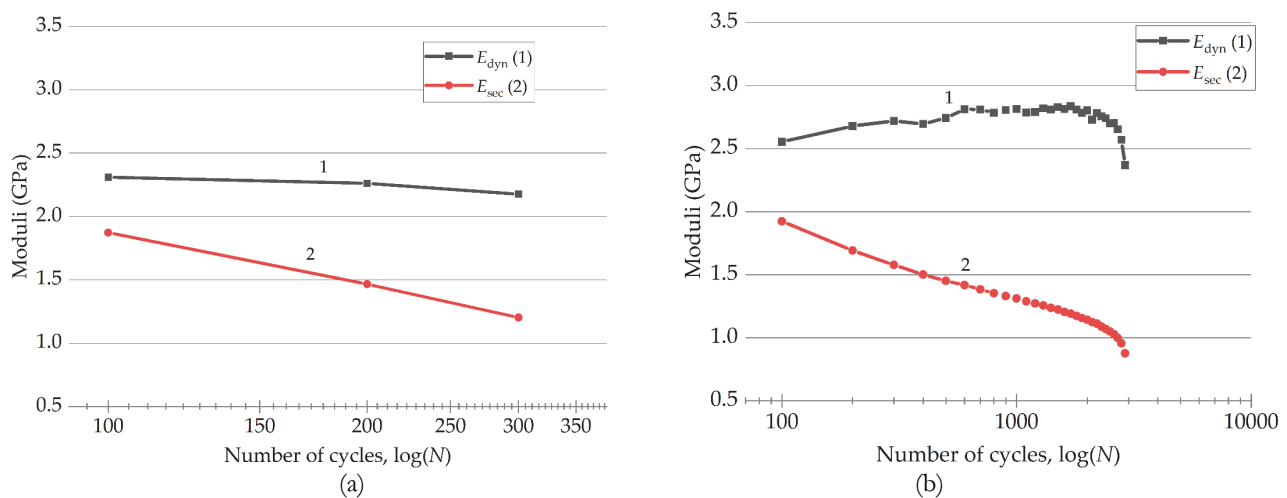

Figure 9: Typical dependences on the dynamic (1) and secant (2) moduli versus the number of cycles at the maximum stains in a cycle of 0.93 σ_{UTS} (a) and 0.90 σ_{UTS} (b).

It was shown in the previous studies by the authors that the E_{sec} secant modulus mainly reflects the development of irreversible strains, while the E_{dyn} dynamic modulus characterizes the accumulation of damage that reduced the specimen stiffness. At the cyclic loads of $0.93 \cdot \sigma_{UTS} = 98$ MPa, the E_{dyn} dynamic modulus reduced slightly (by 5%) down to 2.55 GPa (Fig. 9a, curve 1), reflecting damaging of the specimen. At the same time, a significant decrease in the E_{sec} value from 1.87 down to 1.20 GPa (by 36%) was observed (Fig. 9a, curve 2). During the first 600 cycles, the E_{dyn} dynamic modulus increased by ~260 MPa at the cyclic loads of $0.90 \cdot \sigma_{UTS} = 95$ MPa (Fig. 9b, curve 1). Then, it almost did not change until the last 1000 cycles, when it began to decrease. When the E_{dyn} value reduced down to 2.65 GPa (by 15%), fatigue failure occurred. It is suggested that increasing of the modulus with cyclic loading is due to minor decrease in strain range for tests conducted at 90% of peak load.

The change in the E_{sec} secant modulus (Fig. 9b, curve 2) showed its linear reduction (in logarithmic coordinates) until the last 300 cycles, when the lowering rate accelerated. The total E_{sec} drop was 1.04 GPa (by 54%) for the entire test duration.

TEST RESULTS FOR THE LAMINATED COMPOSITE

Static tension

A stress–strain diagram registered under the static test of the composite is shown in Fig. 10, while its mechanical characteristics are presented in Tab. 2. The curve was characterized by the linear elastic pattern of straining till failure.

Comparing the data in Tabs. 1 and 2, it was concluded that the mechanical properties of the composite exceed those of neat PEEK by a factor of 3.5 in the ultimate tensile strength and by 9 times in the elastic modulus, while its elongation at break was lower by 62 times.
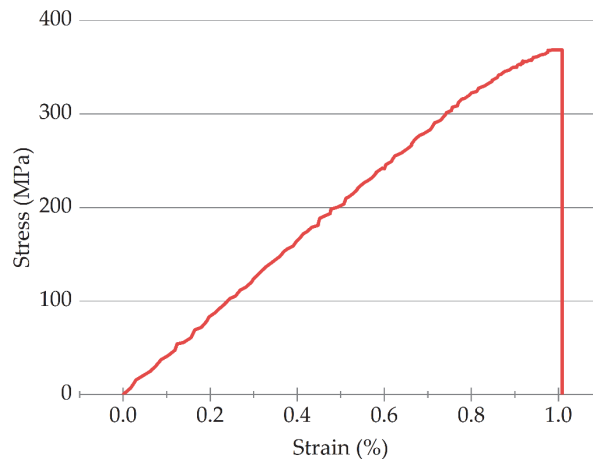

Figure 10. A typical stress–strain diagram for neat PEEK for the laminated composite under the quasi-static tension.

Ultimate tensile strength (MPa), σ_{UTS}	Elastic modulus (GPa), E	Elongation at break (%), ε_f	Yield strength 0.2% (MPa), $\sigma_{0.2}$
370±30	41.2±0.7	1.01±0.12	325±15

Table 2: The mechanical properties of the composite.

The specimen number	The maximum stress σ_{max}, MPa	The maximum stress/ultimate tensile strength ratio, $\sigma_{max}/\sigma_{UTS}$	The number of cycles to failure
1			15116
2	295	~0.8	9608
3			16298

Table 3: The fatigue properties of the composite.

Cyclic tests

Under cyclic loading, the fracture pattern should differ for neat PEEK and the composite, since the reinforced material possessed the minimal viscous strain proportion and was not prone to creep. The results of the fatigue tests of the composite are given in Tab. 3.

There was some variation in the number of cycles to failure, the average value was 13700±3600.

Typical load versus strain responses for PEEK-CF laminate under fatigue are shown in Fig. 11. Note that there was a gradual decrease in the slope of the loop with an increase in the maximum strain in the specimen.
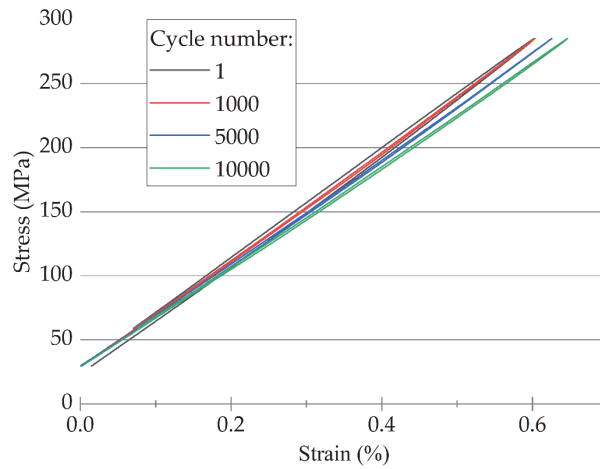

Figure 11: A typical load versus strain response under fatigue of the laminated composite under cyclic loading: $N = 1$; 1000; 5000 and 10000 cycles.

The characteristic patterns of ε_{yy} strain component distribution taken at various number of cycles are given in Fig. 12a. It is seen that gradual damaging of composite in the vicinity of the central hole took place with increasing the number of cycles.
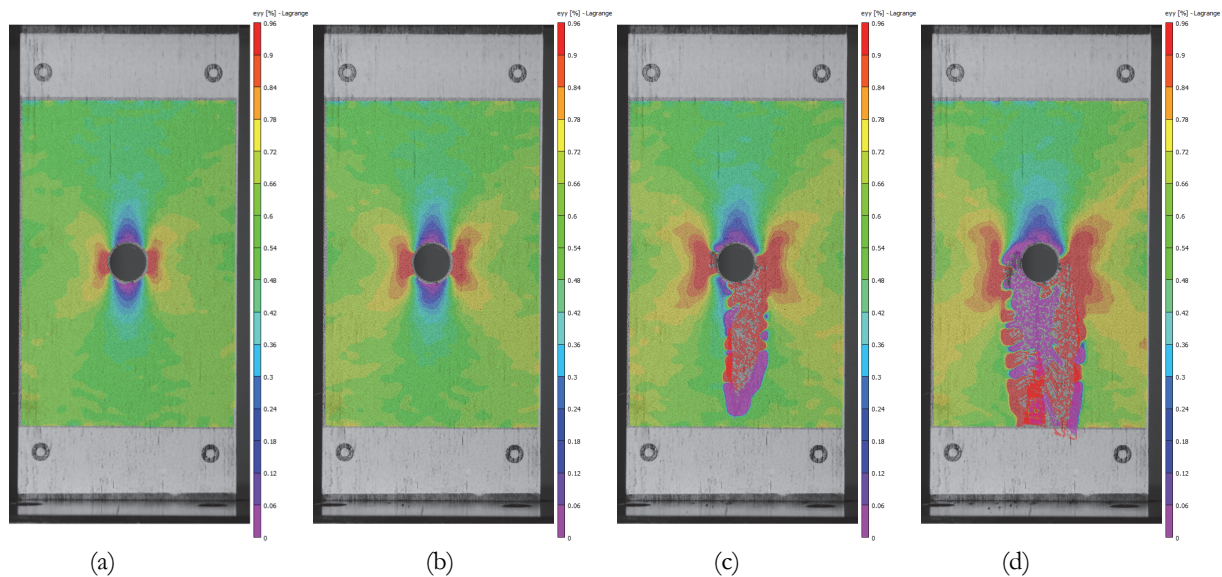

(a)　　　　　　　(b)　　　　　　　(c)　　　　　　　(d)

Figure 12: Characteristic patterns of ε_{yy} strain component distribution taken at various number of cycles; PEEK-CF laminate at the maximum stress in a cycle of 0.8 σ_{UTS}; $N = 1$ cycle (a); 1000 cycles (b); 5000 cycles (c); 10000 cycles (d).

Changes in the maximum and minimum strains, as well as its range for the composite under cyclic loading are shown in Fig. 13. For the maximum load, rising the composite strain was characteristic, associated with a loss of its stiffness as fatigue damage accumulated. At the minimum load, its strain remained at the same level. Respectively, residual strains did not develop. The strain range rose in proportion to its maximum value in a cycle.
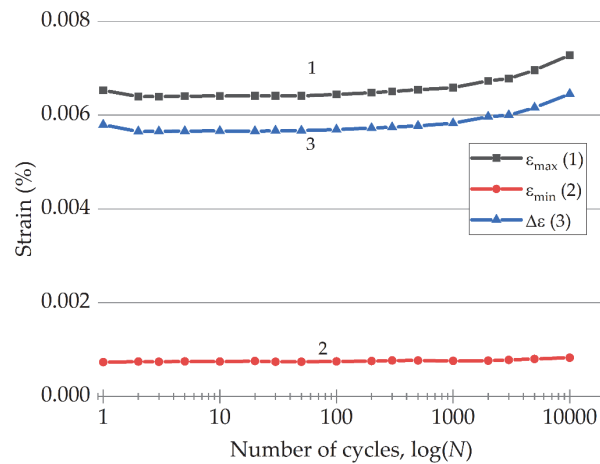
Figure 13: A typical variation pattern of the maximum (1) and minimum (2) strains, as well as its range (3) versus the number of cycles for the PEEK-CF laminated composite.
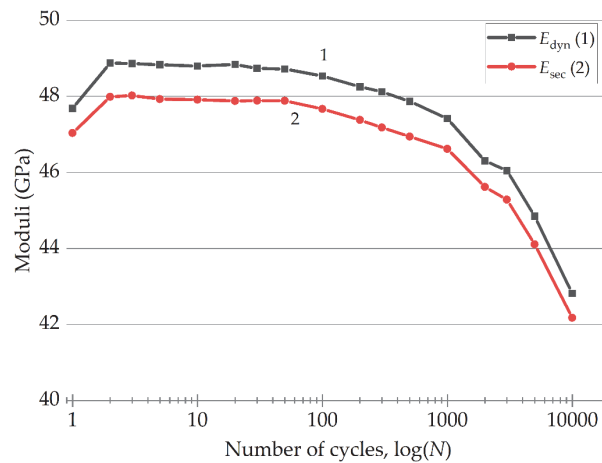

Figure 14: Typical dependences on the changes in the dynamic and secant moduli for the laminated composite under cyclic loading.

Under cyclic loading, the secant and dynamic moduli of the composite changed non-linearly, according to Fig. 14.
Despite negligible variations in the durability, the overall behavior of the analyzed parameters was similar due to the LCF mode of failure. As noted above, the decrease in the secant modulus reflects both the accumulation of damage and the development of cyclic creep. In turn, a decrease in the dynamic modulus indicates a decrease in the stiffness of the specimen. The latter is attributed to the accumulation of fatigue damage. Based on the similar pattern of moduli reduction, it could be concluded that both processes of the scattered damage accumulation and the sample elongation were distributed approximately in equal proportions at the initial test stages.
Before the failure stage, there was an accelerated decline of the dynamic and the secant moduli, which indicated an increase in the damage accumulation rate. In addition, the simultaneous decrease in moduli indicates that damage accumulation is the dominant mechanism compared to creep effects.

CONCLUSIONS

The deformation behavior of both neat PEEK and its laminated composite reinforced with unidirectional carbon fibers was studied under cyclic loading using the DIC method and the calculated parameters of the mechanical hysteresis loops. In these cases, the materials were characterized by different fracture patterns.
For neat PEEK, under cyclic loading under load control mode, there was a significant development of cyclic creep, which was the key fatigue failure mechanism. In contrast, the sample elongation was dominant for the damage accumulation of the PEEK-CF composite.

The parameters of the mechanical hysteresis loops calculated by the DIC method, as quantitative characteristics of property degradation, showed satisfactory sensitivity to the development of various deformation processes (primarily creep and damage accumulation).

Thereby, the DIC method can be effectively implemented for in situ monitoring of the mechanical state of both ductile neat polymers and their rigid fabric- or unidirectionally-reinforced composites.

ACKNOWLEDGMENTS

REFERENCES

[1] Jin, Z., Han, Z., Chang, C., Sun, S., Fu, H. (2022). Review of methods for enhancing interlaminar mechanical properties of fiber-reinforced thermoplastic composites: Interfacial modification, nano-filling and forming technology, Compos. Sci. Technol., 228, pp. 109660, DOI: 10.1016/j.compscitech.2022.109660.

[2] Yao, S.-S., Jin, F.-L., Rhee, K.Y., Hui, D., Park, S.-J. (2018). Recent advances in carbon-fiber-reinforced thermoplastic composites: A review, Compos. Part B Eng., 142, pp. 241–250, DOI: 10.1016/j.compositesb.2017.12.007.

[3] Valino, A.D., Dizon, J.R.C., Espera, A.H., Chen, Q., Messman, J., Advincula, R.C. (2019). Advances in 3D printing of thermoplastic polymer composites and nanocomposites, Prog. Polym. Sci., 98, pp. 101162, DOI: 10.1016/j.progpolymsci.2019.101162.

[4] Hugaas, E., Echtermeyer, A.T. (2021). Filament wound composite fatigue mechanisms investigated with full field DIC strain monitoring, Open Eng., 11(1), pp. 401–413, DOI: 10.1515/eng-2021-0041.

[5] Qiao, Y., Salviato, M. (2020). Micro-computed tomography analysis of damage in notched composite laminates under multi-axial fatigue, Compos. Part B Eng., 187(September 2019), pp. 107789, DOI: 10.1016/j.compositesb.2020.107789.

[6] Battams, G.P., Dulieu-Barton, J.M. (2016). Data-rich characterisation of damage propagation in composite materials, Compos. Part A Appl. Sci. Manuf., 91, pp. 420–435, DOI: 10.1016/j.compositesa.2016.08.007.

[7] Boufaida, Z., Farge, L., André, S., Meshaka, Y. (2015). Influence of the fiber/matrix strength on the mechanical properties of a glass fiber/thermoplastic-matrix plain weave fabric composite, Compos. Part A Appl. Sci. Manuf., 75, pp. 28–38, DOI: 10.1016/j.compositesa.2015.04.012.

[8] Kalteremidou, K.A., Aggelis, D.G., Hemelrijck, D. Van., Pyl, L. (2021). On the use of acoustic emission to identify the dominant stress/strain component in carbon/epoxy composite materials, Mech. Res. Commun., 111, pp. 103663, DOI: 10.1016/j.mechrescom.2021.103663.

[9] Broughton, W.R., Gower, M.R.L., Lodeiro, M.J., Pilkington, G.D., Shaw, R.M. (2011). An experimental assessment of open-hole tension-tension fatigue behaviour of a GFRP laminate, Compos. Part A Appl. Sci. Manuf., 42(10), pp. 1310–1320, DOI: 10.1016/j.compositesa.2011.05.014.

[10] Pannier, Y., Foti, F., Gigliotti, M. (2020). High temperature fatigue of carbon/polyimide 8-harness satin woven composites. Part I: Digital Image Correlation and Micro-Computed Tomography damage characterization, Compos. Struct., 244(March), pp. 112255, DOI: 10.1016/j.compstruct.2020.112255.

[11] Shrestha, R., Simsiriwong, J., Shamsaei, N., Moser, R.D. (2016). Cyclic deformation and fatigue behavior of polyether ether ketone (PEEK), Int. J. Fatigue, 82, pp. 411–427, DOI: 10.1016/j.ijfatigue.2015.08.022.

[12] Berer, M., Major, Z., Pinter, G., Constantinescu, D.M., Marsavina, L. (2014). Investigation of the dynamic mechanical behavior of polyetheretherketone (PEEK) in the high stress tensile regime, Mech. Time-Dependent Mater., 18(4), pp. 663–684, DOI: 10.1007/s11043-013-9211-7.

[13] Eftekhari, M., Fatemi, A. (2016). On the strengthening effect of increasing cycling frequency on fatigue behavior of some polymers and their composites: Experiments and modeling, Int. J. Fatigue, 87, pp. 153–166, DOI: 10.1016/j.ijfatigue.2016.01.014.

[14] Cain, K.J., Glinka, G., Plumtree, A. (2006). Cyclic damage characterization of an off-axis unidirectional graphite bismaleimide composite, Can. Metall. Q., 45(4), pp. 433–440, DOI: 10.1179/cmq.2006.45.4.433.

[15] Hwang, W., Han, K.S. (1986). Fatigue of Composites—Fatigue Modulus Concept and Life Prediction, J. Compos. Mater., 20(2), pp. 154–165, DOI: 10.1177/002199838602000203.

[16] Raphael, I., Saintier, N., Rolland, H., Robert, G., Laiarinandrasana, L. (2019). A mixed strain rate and energy based fatigue criterion for short fiber reinforced thermoplastics, Int. J. Fatigue, 127(April), pp. 131–143, DOI: 10.1016/j.ijfatigue.2019.06.003.

[17] Santharam, P., Marco, Y., Le Saux, V., Le Saux, M., Robert, G., Raoult, I., Guévenoux, C., Taveau, D., Charrier, P. (2020). Fatigue criteria for short fiber-reinforced thermoplastic validated over various fiber orientations, load ratios and environmental conditions, Int. J. Fatigue, 135(December 2019), pp. 105574, DOI: 10.1016/j.ijfatigue.2020.105574.

[18] L Chung, D.D. (2010). Composite Materials: Science and Applications, 2nd Edition, London, Springer London.

[19] Elkin, A., Gaibel, V., Dzhurinskiy, D., Sergeichev, I. (2022). A Multiaxial Fatigue Damage Model Based on Constant Life Diagrams for Polymer Fiber-Reinforced Laminates, Polymers (Basel)., 14(22), DOI: 10.3390/polym14224985.

[20] Movahedi-Rad, A.V., Keller, T., Vassilopoulos, A.P. (2019). Modeling of fatigue behavior based on interaction between time- and cyclic-dependent mechanical properties, Compos. Part A Appl. Sci. Manuf., 124(March), pp. 105469, DOI: 10.1016/j.compositesa.2019.05.037.

[21] Schreier, H., Orteu, J.J., Sutton, M.A. (2009). Image correlation for shape, motion and deformation measurements: Basic concepts, theory and applications, vol. 4, Boston, MA, Springer US.

[22] Bogdanov, A.A., Panin, S. V., Lyubutin, P.S., Eremin, A. V., Buslovich, D.G., Byakov, A. V. (2022). An Automated Optical Strain Measurement System for Estimating Polymer Degradation under Fatigue Testing, Sensors, 22(16), pp. 1–16, DOI: 10.3390/s22166034.

[23] Victrex. Victrex.(2012). Victrex ® PEEK 450G: Material Properties. Available at: www.victrex.com.